# Chapter III-3

# Study of the Elemental Distribution in Ancient Chinese Porcelain Using Synchrotron Radiation X-ray Fluorescence

Y. Y. Huang[1, 2 *], P. L. Leung[2], W. He[1]
[1]*Beijing Synchrotron Radiation Facility, Institute of High Energy Physics, Chinese Academy of Sciences, P. O. Box 918, Beijing 100039, China*
[2]*Department of Physics and Materials Sciences, City University of Hong Kong, Kowloon, Hong Kong, China*
huangyy@mail.ihep.ac.cn

Keywords: porcelain, synchrotron radiation X-ray fluorescence, elemental distribution, suitable spot size

**Abstract**

In this paper, the scanning results of the elemental distribution of an ancient porcelain potsherd in a 200 x 200μm$^2$ area with a 20 x 20μm$^2$ micro X-ray spot were obtained by synchrotron radiation X-ray fluorescence microprobe technique. The elemental distribution of the same porcelain potsherd in the different areas was also measured by using different spots from 100 x 100μm$^2$ to 2 x 6mm$^2$ respectively. The X-ray spot size, the number of measured point and the associated angular distribution of intensity of synchrotron X-ray were carefully investigated in order to find a suitable spot size by which the average elemental distribution of a few measured points can represent the elemental distribution of a whole porcelain ware.

## 1. Introduction

The homogeneity of elemental distribution is an important factor for X-ray fluorescence measurement with a small spot size. As we know, the ancient porcelains were made of several raw materials of ceramics clay following high temperature firing; therefore, the elemental distribution in porcelain is usually not very homogeneous. It becomes an interesting research project to specify how to choose an appropriate X-ray spot size for X-ray fluorescence analysis and how many minimum numbers of measuring points are required in order to acquire the elemental distribution showing a whole porcelain ware. Although some researchers had realized the importance of inhomogeneous element distribution in their



*M. Uda et al. (eds.), X-rays for Archaeology,* 209–216.

analytical areas [1, 2, 3, 4], no detailed study related to ancient porcelain measurement by X-ray fluorescence analysis was reported until recently.

In the work of reference [1], it was pointed out that there is non-homogeneity of the element distribution in and under the surface of porcelain. In the surface, the solution is to choose a bigger size of X-ray spot or take a mean of the different measurement points by using a smaller X-ray spot. However, it is difficult to solve the problem under surface. In this paper we mainly focused on the surface distribution of elements.

The microbeam scanning analysis is an important way to solve this problem. In this study, the elemental homogeneity measurement of two-dimension distribution of ancient porcelain was performed by synchrotron radiation X-ray fluorescence (SRXRF) analysis. The results of homogeneity for a typical ancient porcelain sherd are presented.

## 2. Experimental facility

Synchrotron radiation is a powerful advanced light source compared to conventional X-ray tube radiations, and has many unique properties, such as high intensity, natural collimation, well-defined polarization, wide spectral range and energy tunability. SRXRF technique is a non-destructive and free contact analytical method, and especially large specimen testing can be performed in air environmental condition. It is very suitable for valuable ancient porcelain analysis. Measurements for this paper were carried out at the XRF experimental station at the Beijing Synchrotron Radiation Facility (BSRF) [5, 6].

## 3. Experimental results and discussion

### 3.1 MICROBEAM SCANNING ANALYSIS OF MAJOR AND TRACE ELEMENTS

The experimental specimen used here is a sherd of celadon porcelain made in the South Song Dynasty. In the experiment the scanning area is 200x200μm$^2$, the micro beam size is 20x20μm$^2$. The white spectrum of synchrotron radiation was used; the energy range is 3-30 KeV at Beam line 3W1A of BSRF. The scanning distributions of the major element Ca and Fe, as well as the trace element Cu, Rb, and Zr of glaze of the porcelain sherd are shown in the Fig.1. X and Y-axis indicate the relative position of the scanning beam; Z-axis indicates the relative elemental content. Fig.1 shows that the elemental distribution of the porcelain sherd is inhomogeneous, especially for the element Zr in the analytical area. This special non-homogeneity distribution of element Zr was little mentioned; this may be because the sensitivity of the convention XRF and electron probe analytical techniques is usually lower than SRXRF in such a small analytical area. Similar results of non-homogeneity distribution of Zr element from other Chinese porcelain sherds made in the different dynasties were often found in our research work. For

the other major and trace elements, similar results of inhomogeneous elemental distribution were also observed, here only a few typical results are shown.

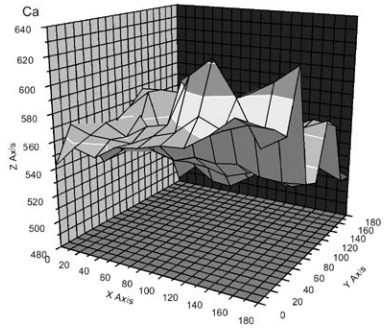


*Fig1*.a:element Ca

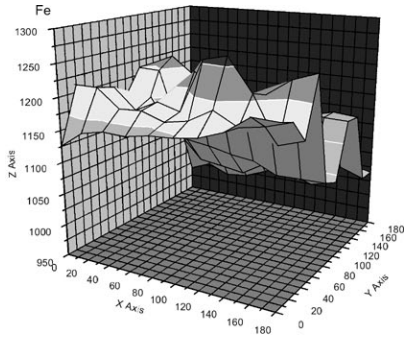


*Fig1*.b: element Fe

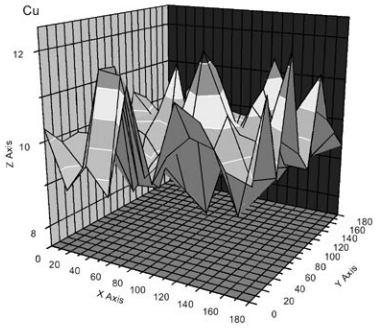


*Fig1*.c: element Cu

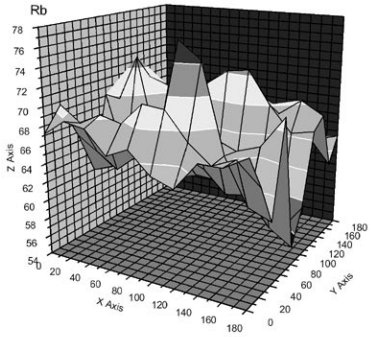


*Fig1*.d: element Rb

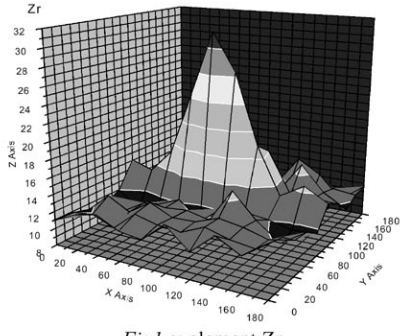


*Fig1*.e: element Zr

*Fig. III-3-1*.The scanning distributions of the major element Ca and Fe, as well as the trace element Cu, Rb, and Zr of glaze of the porcelain sherd, a: element Ca, b: element Fe, c: element Cu, d: element Rb, e: element Zr. X and Y-axis indicate the relative position of the scanning beam; Z-axis indicates the relative elemental content.

## 3.2 BEAM SIZE AND ANGULAR DISTRIBUTION EFFECT OF SYNCHROTRON RADIATION INTENSITY

In the experiment we measured five different positions of the glaze of the same porcelain sherd, with different micro beam sizes from 100x100μm$^2$ to 400x400μm$^2$ (white spectrum 3-30 KeV, 4W1A beam line) and from 2x2 to 2x6 mm$^2$ (monochromatic spectrum, 10KeV, 4W1B beam line). That is, we first measured five different positions of the glaze of the same porcelain sherd with the micro beam size of 100x100μm$^2$, and then the other five different positions with 200x200μm$^2$, and so on. The mean values of the five different position (five times) measurements and their standard deviations of elemental relative contents were determined and shown in Fig. 2a, 2b and 2c, where vertical axis indicates relative elemental contents per unit beam size area.

Because of the angular distribution effect of SR intensity itself in vertical direction [7], i.e. the SR intensity decreased with the increase of the distance from the orbit plane of electron beam in the storage ring of the accelerator [8, 9]. Therefore, the mean values per unit beam size area of the five different position measurements decreased when the beam size changed from 100x100μm$^2$ to 400x400μm$^2$ in the Fig. 2a. In our experiment the orbit plane was in the middle of the vertical slit, that is, it was in the middle of the vertical direction of the beam size. The same cases occur in Fig. 2b and 2c, where the horizontal slit was fixed, only the vertical slit changed from 2 to 6mm, i.e. the beam size changed from 2x2 to 2x6 mm$^2$.

In order to further explain this phenomenon of angular distribution in Fig. 2a, 2b and 2c, especially in vertical direction, a reference experimental result was determined by measuring a homogeneous stainless steel film standard specimen (SS4) [10] with different X-ray spot sizes. The result is shown in Fig. 2d; the vertical axis indicates relative elemental contents per unit beam size area. The curve is the first order exponential decay fitting result. It was shown that the SR intensity decreased with the increase of the distance from the orbit plane of electron beam in the storage ring of the accelerator and also observes the exponential decay. It was shown that the decay of the curves in Fig. 2a, 2b, and 2c correspond with the one in Fig. 2d. It can also be seen that the standard deviations in Fig. 2a, 2b and 2c decreased with the beam size increase. It means that with the same measuring times the larger the beam size is, the better the mean measurement value.

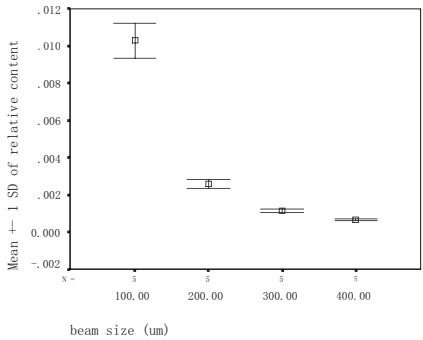


*Fig III-3-2a.* The mean values (square sign) of five different position measurements (N=5) and their standard deviations (SD) of the relative contents of Fe element are shown. X-axis indicates the measuring times (upper) and beam size (bottom).

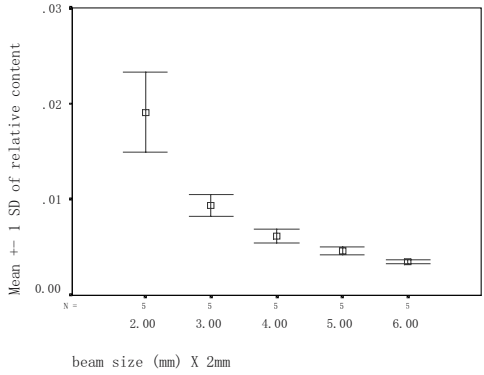


*Fig.III-3-2b*. The mean values (square sign) of five different position measurements (N=5) and their standard deviations (SD) of the relative contents of Ca element are shown. X-axis indicates the measuring times (upper) and beam size (bottom).

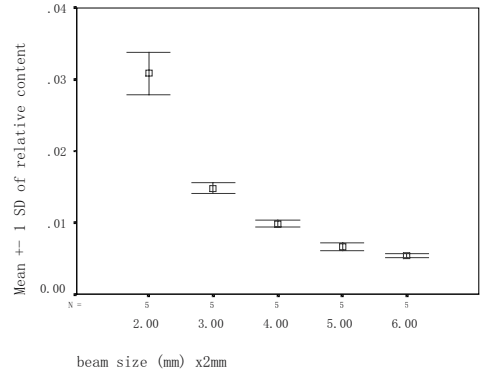


*Fig. III-3-2c*. The mean values (square sign) of five different position measurements (N=5) and their standard deviations (SD) of the relative contents of Fe element are shown. X-axis indicates the measuring times (upper) and beam size (bottom).

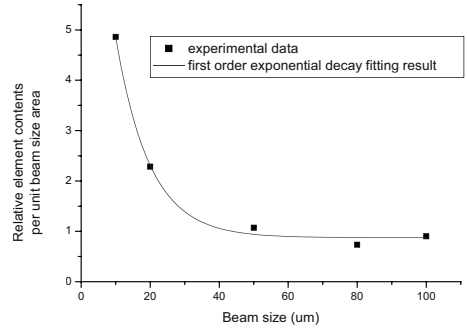


*Fig. III-3-2d*. The vertical axis indicates relative elemental contents per unit beam size area for elemental iron, horizontal axis is the beam size of the vertical slit, and all the beam spot are the squares.

## 3.3 RELATION BETWEEN THE SPOT SIZE AND THE NUMBER OF THE TESTING POINT

As the description above in the section 3.1, the scanning area in the experiment is 200x200μm$^2$, the micro beam size is 20x20μm$^2$ . The beam was scanned one by one without overlapping and spacing on the surface of the porcelain. That is, there are 100 different positions (square areas) each one with size 20x20μm$^2$. The relative elemental contents in each one position were determined and are shown in Fig. 1.

Therefore, there are also 25 different positions (square areas,) each one with size 40x40μm$^2$ for the scanning area of 200x200μm$^2$. Each bigger square with size 40x40μm$^2$ is composed of four adjacent smaller squares each one with size 20x20μm$^2$. The relative elemental contents in each one with size 40x40μm$^2$ can be obtained by adding those of the four adjacent smaller squares each one with size 20x20μm$^2$. In the same way, there are also 4 different positions (square areas) each one with size 100x100μm$^2$ for the scanning area of 200x200μm$^2$. The relative elemental contents in each one with size 100x100μm$^2$ can be obtained.

The 40x40μm$^2$ and 100x100μm$^2$ can be regarded as a bigger beam spot size for the scanning area of 200x200μm$^2$ respectively. Therefore, the mean values and their standard deviations of the elemental relative contents could be obtained by averaging the different measuring positions (square areas, here 100, 25 and 4 respectively), which are shown in Table 1 and Fig. 3a for calcium as well as Fig. 3b for iron. In this way the problem of the beam size and the angular distribution effect of synchrotron radiation intensity can be avoided. The relation between the spot size and number of the testing point becomes simple.

As shown in the Table 1 and the Fig. 3, the mean values of the elemental relative contents are almost the same for calcium and the same for iron when the beam size increases. Meanwhile the standard deviations become smaller and smaller with increasing beam size. That means that the measuring results of element calcium and iron are already accepted when the beam size 20x20μm$^2$ is used for the analytical area of 200x200μm$^2$, but it needs to measure 100 different positions. However, if a larger spot size is used, for example, 100x100μm$^2$, only 4 different testing points are enough and the measuring precision is higher. Therefore, the beam size of 100x100μm$^2$ can be regarded as a suitable spot size by which the average elemental distribution of the four measured points can represent the elemental distribution of the materials.

*Table III-3-1*. The mean relative elemental contents per unit beam size area and their standard deviations.

| beam size (um) | 20 | 40 | 100 |
|---|---|---|---|
| number of square area | 100 | 25 | 4 |
| Ca mean value | 2.8352 | 2.8360 | 2.8350 |
| Ca standard deviation | 0.1727 | 0.1598 | 0.1162 |
| Fe mean value | 1.3776 | 1.3776 | 1.3776 |
| Fe standard deviation | 0.0792 | 0.0746 | 0.0567 |

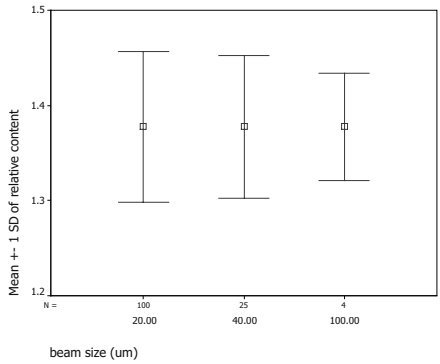


*Fig. III-3-3a*. The mean values (square sign) and their standard deviations (SD) of the relative contents of element Ca are shown. X-axis indicates the measuring times (upper) and beam size (bottom), Y-axis indicates the relative elemental content per unit beam size area.

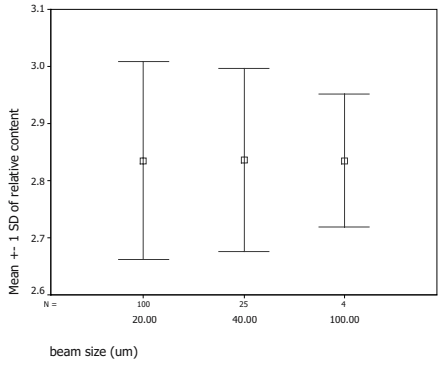


*Fig. III-3-3b.* The mean values (square sign) and their standard deviations (SD) of the relative contents of element Fe are shown. X-axis indicates the measuring times (upper) and beam size (bottom), Y-axis indicates the relative elemental content per unit beam size area.

## Conclusion

Elemental distribution is inhomogeneous for ancient Chinese porcelain, such as the celadon porcelain measured above, especially for element Zr. When measuring the sample, if the beam size is changed, especially in the vertical direction, the angular distribution effect of the synchrotron radiation intensity should be considered. For obtaining the accepted average measuring value of elemental contents, less testing points is needed and higher precision can be obtained when the larger beam size is used. One suitable beam spot size was determined. By using this beam size the average elemental distribution of a few measured points represents the elemental distribution of a whole porcelain ware.

**Acknowledgements**

The work described in this paper was partially supported by a grant from the City University of Hong Kong (Project No.7001104), and the experiments were carried out at the Beijing Synchrotron Radiation Facility.

## References

[1]. He Wenquan, and Xiong Yingfei, (1999) *The Non-Destructive Analysis of Ancient Ceramics*, in Guo Jingkun (eds), The Proceedings of the 1999 International Symposium on Ancient Ceramics-its Scientific and Technological Insights, Shanghai Scientific and Technical Reference Publishers, Shanghai, China, pp563-567.

[2]. M. Mantler and M. Schreiner, (2000) X-ray Fluorescence Spectrometry in Art and Archaeology, *X-ray Spectrometry* **29**, 3-17.

[3]. P. Wobrauschek, G. Halmetshclager, S. Zamini, C. Jokubonis, G. Trnka and M. Karwowski, (2000) Energy-Dispersive X-ray Fluorescence Analysis of Celtic Glasses, *X-ray Spectrometry* **29**, 25-33.

[4]. K. Janssens, G. Vittiglio, I. Deraedt, A. Aerts, B. Vekemans, L. Vincze, F. Wei, I. Deryck, O. Schalm, F. Adams, A. Rindby, A. Knochel, A. Simionovici and A. Snigirev, (2000) Use of Microscopic XRF for Non-destructive Analysis in Art and Archaeometry, *X-ray Spectrometry* **29**, 73-91.

[5]. Y. Y. Huang, K. F. Li, W. He, G. C. Li and K. X. Lin, (2001) Single Fluid Inclusion Study by SRXRF Microprobe, *Nuclear Instruments and Methods in Physics Research* A **467-468 ,**1315-1317.

[6]. Y. Y. Huang, J. X. Lu, R. G. He, L. M. Zhao, Z. G. Wang, W. He and Y. X. Zhang, (2001) Study of Human Bone Tumor Slice by SRXRF Microprobe, *Nuclear Instruments and Methods in Physics Research* A **467-468,** 1301-1304.

[7]. A. Iida, (2000) Instrumentation for μ-XRF at Synchrotron Radiation Sources, in Koen H. A. Janssens, Freddy C.V. Adams and Anders Rindby (eds), *Microscopic X-ray Fluorescence Analysis*, John Wiley & Sons Ltd, pp.121-123.

[8]. Tang Esheng, Huang Yuying, Wu Yingrong and Yi Futing (1998) Radiation Character of 3W1 Permanent Magnet Multipole Wiggler, *High Energy Physics and Nuclear Physics*, (Chinese), **22,** 951-954.

[9]. Esheng Tang, Yonglian Yan, Shaojian Xia, Peiwei Wang, Futing Yi, Yuying Huang, Jin Liu and Mingqi Cui (1998) New Wiggler Beam Line at BSRF, *Journal of Synchrotron Radiation*, **5,** 530-532.

[10]. H. Shao and Q. Xu (1995) *Nucl. Instr. And Meth. In Phys. Res*.B **104** , 201-203.